

# Fault-Tolerant Operating Analysis of a Quad-Inverter Multiphase Multilevel AC Motor Drive

G. Grandi, Y. Gritli, F. Filippetti, and C. Rossi,

**Abstract** -- This paper investigates a new fault-tolerant strategy of a multi-phase multi-level ac motor drive. The proposed approach is based on four conventional 2-level three-phase voltage source inverters (VSIs) supplying the open-end windings of a dual three-phase motor (asymmetric six-phase machine), quadrupling the power capability of a single VSI with given voltage and current ratings.

The developed fault-tolerant control algorithm is able to generate multi-level voltage waveforms, equivalent to the ones of a 3-level inverter, and to share the total motor power among the four dc sources within each switching period. The investigated ac motor drive has been numerically implemented, under healthy and for three degraded modes of the system, are given to prove the effectiveness of the whole strategy.

**Index Terms**--Dual three-phase motors, space vector modulation, multilevel inverters, multiphase motor drives, fault-tolerance.

## I. INTRODUCTION

**F**AULT-TOLERANCE in motor drive systems is a key item in high power transport applications, where availability and reliability of operation are mandatory. Specifically, for this type of application, induction motors operate continuously under time-varying operating conditions, requiring rapid speed variation and frequent stop / starting. Subsequently, the circuits are regularly subjected to abuse of over-current surge and voltage overswings. Investigations on different failure modes in induction motors done by industrials and experts have revealed that 21% of motor failures are related to the stator windings [1]. Several phenomenon can affect its reliability, such as mechanical and/or thermal stress, leading to severe failure modes as inter-turn short-circuits, line-to-line, line-to-ground, multiphase line-to ground and multiphase faults. A detailed analysis of this type of faults and its modes of propagation and diagnosis can be found in [1-3].

As advanced solution, among various strategies presented in literature for fault-tolerant operating condition, multi-phase ac machines technologies have been widely recognized as viable solutions in the field [4]. More specifically, multi-phase drives are very advantageous in high power transport applications, thanks to its inherent active redundant structure, which improve considerably the system reliability. It takes only two phases to create a fundamental mmf

distribution rotating at the supply frequency, so a machine with  $m$  phases can continue to operate at reduced power in a controlled manner, with  $m-2$  phases open circuit. Therefore, multi-phase inverters together with multi-phase ac machines have been proved as a potential alternative, allowing high power ratings with current limited devices [4-5]. Other investigations have focused their efforts on multi-level converters. Mainly, these converters are advantageous in terms of high voltages that can be synthesized using sources and switching devices with lower voltage values, with the additional benefit of a reduced harmonic distortion and lower  $dv/dt$  in the output voltages [6-7].

Several other topologies, with passive or/and active semiconductors have been proposed for the same purposes. However, its lower reliability, still remain their major drawback. A recent reliability investigation of converter topologies, has revealed that its estimated mean time between failures (MTBFs) is of about 2 years [8]. Anyway, among these modern inverter topologies, the conventional 2-level three-phase voltage source inverter still remains a mature technology. However, all types of inverters still vulnerable to different potential anomalies, leading to an imminent total failure. A large survey on converter reliability has shown that 31-37.9 % of all converters failures are caused by power parts [9-10]. Exhaustive details about the main failure mechanisms in modern power modules with insulated gate bipolar transistor devices for high-power applications can be found in [11]. More recently, another survey on converters has revealed that power devices, capacitors and gate control are the most potential source of failures [12]. In this sense, innovative topologies based on a proper arrangement of conventional 2-level three-phase voltage source inverters (VSIs) to realize both multi-phase [13-14] and multi-level [15-18] inverters, have been investigated. The reduced cost of both converter and motor due to conventional slot/winding configurations, and modularity of the whole conversion structure, with high reliability in power layout, are the main advantages of such topologies. Motivated by the above performances, and considering the low reliability of the commercial inverters becoming more and more integrated, which reduce considerably its maintainability or reconfiguration [19], a novel structure based on a dual three-phase open-ends winding motor (asymmetric six-phase induction machine) has been considered in this paper. The power supply consists of four standard 2-level three- phase VSIs having insulated

---

G. Grandi, Y. Gritli, F. Filippetti and C. Rossi are with the University of Bologna, Department of Electrical Engineering, Viale Risorgimento, Bologna – ITALY. Phone : +39 051 2093 564, Fax: +39 051 2093 588. (e-mail: gabriele.grandi@unibo.it, yasser.gritli@unibo.it, fiorenzo.filippetti@unibo.it, claudio.rossi@unibo.it).

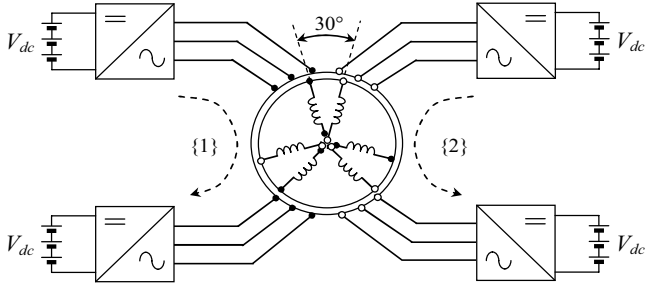


Fig. 1. Schematic diagram of the proposed multi-phase multi-level ac motor drive consisting in four voltage source inverters supplying a dual three-phase machine with open-end windings.

dc sources to prevent circulation of zero-sequence current components and improving the reliability. A schematic diagram of the whole system is given in Fig. 1. Note that the structure is easy scalable to nine, twelve or higher number of phases multiple of three. A modulation strategy has been proposed to regulate each couple of 2-level VSIs such as a 3-level inverter, providing proper multi-level voltage waveforms for each three-phase stator winding. Furthermore, the proposed control algorithm allows total motor power to be shared among the four dc sources with three degrees of freedom, leading to a combination/extension of the power sharing principles given in [20] and [21]. In this sense, the proposed contribution is devoted to analyze how to exploit the inherent redundancy provision of the used quad-inverter, in different emergency cases where one, two or three inverters fail.

## II. DUAL THREE-PHASE INDUCTION MOTOR DRIVE UNDER HEALTHY CONDITION

Multiple space vectors are considered to represent the variables of the whole six-phase system consisting of the dual three-phase machine supplied by four insulated three-phase VSIs. In particular, the asymmetric six-phase space vector transformations introduced in [13, 14] are considered. The representation of the proposed multi-phase multi-level induction motor drive shown in Fig. 1, in terms of three-phase space vectors, under healthy condition leads to the schematic equivalent circuit of Fig. 2. The behavior of the dual three-phase induction machine having sinusoidal distributed stator windings can be described in terms of multiple space vectors by the following equations, written in a stationary reference frame [14]:

$$\bar{v}_{S1} = R_S \bar{i}_{S1} + \frac{d\bar{\Phi}_{S1}}{dt}, \quad \bar{\Phi}_{S1} = L_{S1} \bar{i}_{S1} + M_1 \bar{i}_{R1}, \quad (1)$$

$$0 = R_R \bar{i}_{R1} - j p \omega_m \bar{\Phi}_{R1} + \frac{d\bar{\Phi}_{R1}}{dt}, \quad \bar{\Phi}_{R1} = M_1 \bar{i}_{S1} + L_{R1} \bar{i}_{R1}, \quad (2)$$

$$\bar{v}_{S5} = R_S \bar{i}_{S5} + \frac{d\bar{\Phi}_{S5}}{dt}, \quad \bar{\Phi}_{S5} = L_{S\ell} \bar{i}_{S5}, \quad (3)$$

$$T = 3p M_1 \bar{i}_{S1} \cdot j \bar{i}_{R1}, \quad (4)$$

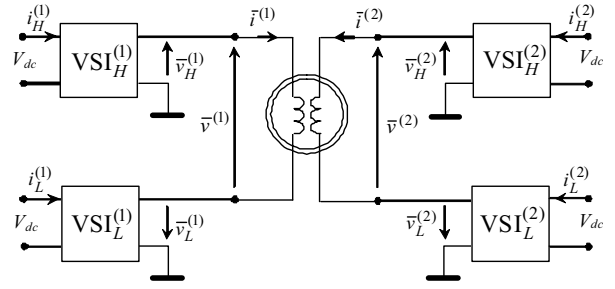


Fig. 2. Equivalent circuit of the whole induction motor drive in terms of three-phase space vectors, under healthy quad-inverter condition.

where  $p$  is the pole pairs number,  $\omega_m$  is the rotor angular speed, and the subscripts  $S$  and  $R$  denote stator and rotor quantities, respectively. It should be noted that  $\bar{i}_{S1}$  and  $\bar{i}_{R1}$  are responsible for the sinusoidal spatial distribution of the magnetic field in the air gap, whereas  $\bar{i}_{S5}$  does not contribute to the air gap field. In dual three-phase induction motor drives, the reference values of the  $d_1$ - $q_1$  components of the stator currents in a synchronous reference frame,  $i_{1d,ref}$  and  $i_{1q,ref}$ , are determined on the basis of flux and torque commands, respectively [20]. The  $d$ -axis of synchronous reference frame is aligned with the rotor flux, displaced by angle  $\vartheta$  with respect to the  $d$ -axis stationary reference frame.

In the proposed system, the power sharing among the four dc sources is characterized by three degrees of freedom [22]. The first one concerns the power sharing between the two three-phase windings {1} and {2}, whereas second and third ones are related to the power sharing between the two inverters H and L which supply each three-phase winding.

As introduced in [5] and developed in [14], with a good approximation, the total motor power  $P$  between the two three-phase windings {1} and {2} as:

$$P = P^{(1)} + P^{(2)}, \quad (5)$$

$$\begin{cases} P^{(1)} = \frac{3}{2} \bar{v}^{(1)} \cdot \bar{i}^{(1)} \\ P^{(2)} = \frac{3}{2} \bar{v}^{(2)} \cdot \bar{i}^{(2)} \end{cases} \quad (6)$$

where  $\bar{v}^{(1)}$  ( $\bar{v}^{(2)}$  respectively) can be synthesized as the sum of the voltages  $\bar{v}_H^{(1)}$  and  $\bar{v}_L^{(1)}$  generated by VS1\_H^(1) and VS1\_L^(1), respectively, leading to

$$\begin{cases} \bar{v}^{(1)} = \bar{v}_H^{(1)} + \bar{v}_L^{(1)} \\ \bar{v}^{(2)} = \bar{v}_H^{(2)} + \bar{v}_L^{(2)} \end{cases} \quad (7)$$

In terms of averaged values within the switching period, the power of the first three-phase stator winding {1} can be expressed as:

$$P^{(1)} = \frac{3}{2} \bar{v}^{(1)} \cdot \bar{i}^{(1)} = P_H^{(1)} + P_L^{(1)}, \quad (8)$$

where  $P_H^{(1)}$  and  $P_L^{(1)}$  are the individual powers from the two inverters, which can be expressed as follow:

$$\begin{cases} P_H^{(1)} = \frac{3}{2} \bar{v}_H^{(1)} \cdot \bar{i}^{(1)} \\ P_L^{(1)} = \frac{3}{2} \bar{v}_L^{(1)} \cdot \bar{i}^{(1)} \end{cases} \quad (9)$$

With similar considerations, the powers to the second three-phase stator winding {2} can be expressed as:

$$P^{(2)} = \frac{3}{2} \bar{v}^{(2)} \cdot \bar{i}^{(2)} = P_H^{(2)} + P_L^{(2)}. \quad (10)$$

where

$$\begin{cases} P_H^{(2)} = \frac{3}{2} \bar{v}_H^{(2)} \cdot \bar{i}^{(2)} \\ P_L^{(2)} = \frac{3}{2} \bar{v}_L^{(2)} \cdot \bar{i}^{(2)} \end{cases} \quad (11)$$

Finally, substituting (8) and (10) in (1) the total motor power  $P$  between the two three-phase windings {1} and {2} can be expressed as, leading to the torque versus speed pattern, presented in Fig. 3.

$$P = \frac{3}{2} (\bar{v}_H^{(1)} \cdot \bar{i}^{(1)} + \bar{v}_L^{(1)} \cdot \bar{i}^{(1)} + \bar{v}_H^{(2)} \cdot \bar{i}^{(2)} + \bar{v}_L^{(2)} \cdot \bar{i}^{(2)}) \quad (12)$$

Once the reference voltage vectors  $\bar{v}^{(1)}$  and  $\bar{v}^{(2)}$  for the two couples of inverters are determined, a proper multilevel SVM algorithm must be applied to satisfy the power sharing low between the two windings developed in [14]. Due to the symmetry of the outer hexagon, the analysis can be restricted to one of its six sectors (i.e., OAB in Fig. 4), similarly to the case of conventional three-phase SVM algorithm.

Furthermore, the main triangle OAB is divided in four identical equilateral triangles. The reference voltage  $\bar{v}^{(1)}$  lays in one of these triangles, leading to four relevant cases. By the basic SVM principle, the components  $\bar{v}_H^{(1)}$  and  $\bar{v}_L^{(1)}$  can be generated by selecting adjacent vectors.

The switch configurations corresponding to these vectors cannot be applied in an arbitrary sequence if proper multilevel voltage waveforms are desired, i.e., the reference voltage  $\bar{v}^{(1)}$  should be generated by using the nearest three vectors approach (NTV) [21]. For this purpose, the method introduced in [18] has been implemented. The same considerations are valuable for the voltage reference  $\bar{v}^{(2)}$ . The torque versus speed patten depicted in Fig. 3, with the voltage space vectors (Fig. 4) generated by the inverters H and L for both stator windings {1} and {2}, Under healthy condition, will be considered as a reference for the degraded systems that will be analyzed in the next section. In order to

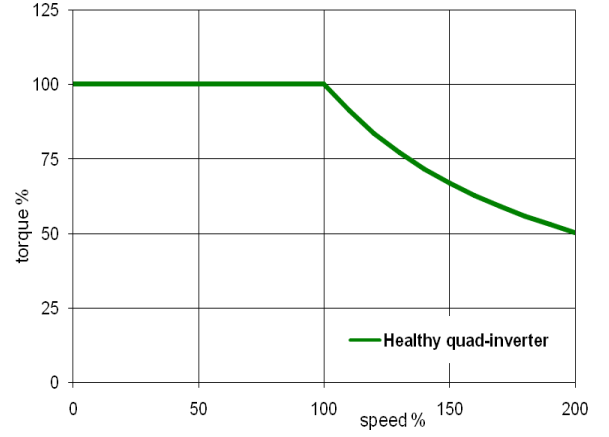


Fig. 3. Torque versus rotor speed under healthy quad-inverter condition

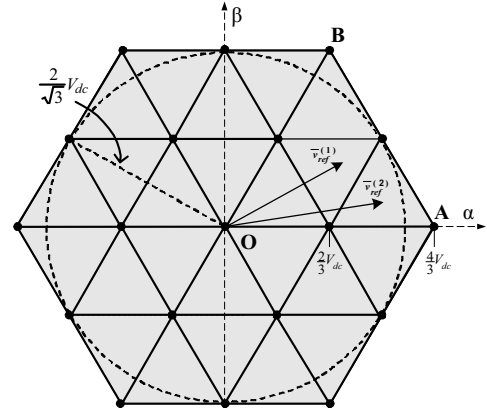


Fig. 4. Plot of voltage space vectors generated by inverters H and L for both the stator windings {1} and {2}, under healthy quad-inverter condition.

verify the effectiveness of the proposed control strategy, under healthy and several failure conditions of inverters, the whole system has been designed and numerically tested by means of the PLECS simulation package in the MATLAB environment. For the induction motor, the model presented in Section II has been implemented using the parameters given in Appendix. The value of the four dc bus voltages ( $V_{dc}$ ) is set to 155 V and a switching frequency of 5 kHz is selected.

### III. FAULT-TOLERANCE ANALYSIS

Actually, integrated cooling technologies are widely deployed in commercial inverters for high power applications devoted to transport systems. The use of this type of technology satisfies new demands in term of ease-of-use, miniaturization and compactness in transport systems. However, the non-maintainability due to the compact packaging and the reduced thermal dissipation justifies the reduced reliability of the inverters [8], [11], [19].

Independently to the technology adopted, the inverters are still subjected to several potential failures due to;

- dc-link electrolytic capacitor,
- dc bus voltage sensor,

- power semiconductor (short circuit or open circuit),
- control circuit,
- driver circuits,

leading inevitably to the total or partial damage, which propagate rapidly, leading to severe degrees of damage for the whole system. For these reasons, whenever one between the four 2-level three-phase voltage source inverters is affected by the above failures, the concerned inverter is considered as totally damaged and must be removed.

The failed inverter is disconnected from both the motor and the battery source using bypass switches. Then, the developed control system is adapted in a manner that the AC motor drive machine still continues to operate in post-fault inverter conditions.

More than one singular inverter failure condition could be treated in the same way. In the analysis presented below, one, two and three failure conditions, for the used quad-inverter configuration, are detailed and commented.

#### A. Control strategy under one failed inverter condition

In the first case, the impact of one failed inverter on the operability of the system is analyzed reference is made to the scheme of Fig.5.

As previously mentioned, the failed inverter, must be disconnected from both the motor and the battery source, using bypass switches with an appropriate choice of threshold. Furthermore, the three motor wires must be short-circuited to allow current circulation. The open winding configuration now collapse in a traditional three-phase star connection for a three-phase winding. The post fault topology reconfiguration for this case leads to:

$$v_L^{(2)} = 0 \quad (13)$$

It is worth noting that for this post-fault topology, the use of  $VSI_H^{(2)}$  with either  $VSI_H^{(1)}$  or  $VSI_L^{(1)}$  leads to the same operating performances of the motor. Eventually, the use of  $VSI_H^{(1)}$  or  $VSI_L^{(1)}$  for an active redundancy is not recommended to reduce the switching losses. However, a passive redundancy provision of one inverter for the winding {1} improve considerably the reliability of the post-fault configuration in emergency circumstances.

Subsequently, under this degraded condition and taking into account the equations (7) with (13), the total motor power  $P$  between the two three-phase windings {1} and {2}, expressed by (12) under healthy condition, becomes:

$$P = \frac{3}{2} \left( \bar{v}_H^{(1)} \cdot \bar{i}^{(1)} + \bar{v}_L^{(1)} \cdot \bar{i}^{(1)} + \bar{v}_H^{(2)} \cdot \bar{i}^{(2)} \right) \quad (14)$$

Under post-fault condition, the system is able to continue the operation, with high torque performances, as for a healthy system for the speed range from 0 to 50% of the rated speed. Above 50% of the loaded speed, the system still remains operable but with reduced torque as depicted in Fig. 6.

This is mainly due to the loss of voltage occurring after the

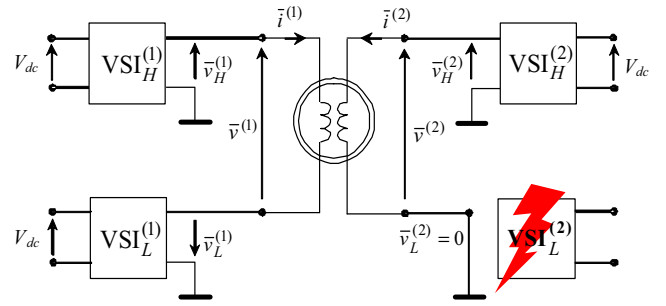


Fig. 5. Equivalent circuit of the whole induction motor drive in terms of three-phase space vectors, under one failed inverter.

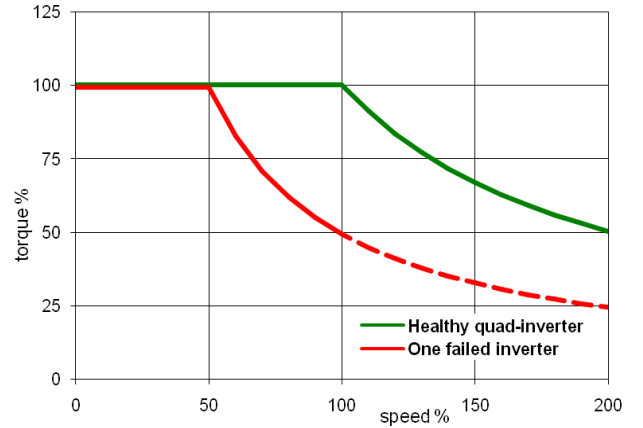


Fig. 6. Torque versus rotor speed under healthy and one failed inverter conditions.

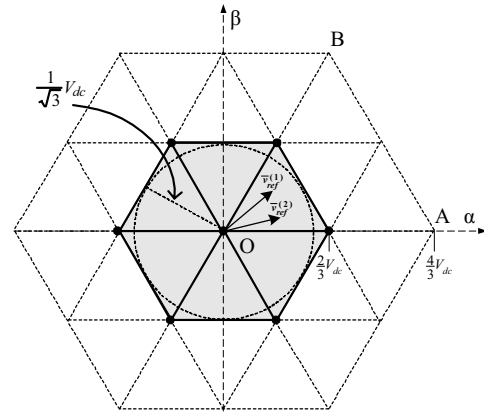


Fig. 7. Plot of voltage space vectors generated by inverters H and L for both the stator windings {1} and {2}, under one failed inverter.

disconnection of the failed inverter, as depicted in Fig. 5 and expressed by (14). Once the reference voltage vectors  $\bar{v}^{(1)}$  and  $\bar{v}^{(2)}$  for the three healthy inverters  $VSI_H^{(1)}$ ,  $VSI_L^{(1)}$ , and  $VSI_H^{(2)}$  are determined, the multilevel SVM algorithm, is applied to satisfy the power sharing between the three considered inverters. Eventually, under these circumstances, the system allows the degraded quad-inverter, allow the supply of the motor as a classical two level inverter. The corresponding space vectors generated and the concerned area of operation are depicted in Fig. 7. It is important to note that under this post fault configuration, the system is able to run for a prolonged long time period without overheating neither on the motor, nor on the inverters.

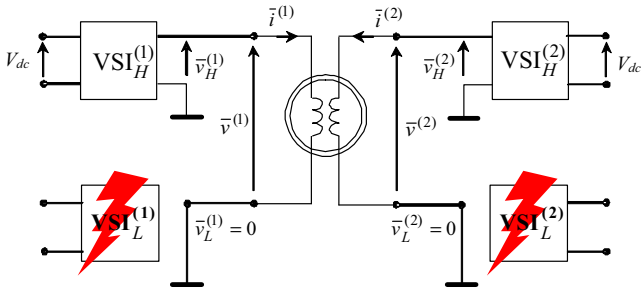


Fig. 8. Equivalent circuit of the whole induction motor drive in terms of three-phase space vectors, under two failed inverters, one for each stator windings {1} and {2}.

Naturally, the same considerations are valuable, even it is the failure case of the inverter VSI<sub>H</sub><sup>(2)</sup>, VSI<sub>H</sub><sup>(1)</sup> or VSI<sub>L</sub><sup>(1)</sup>.

### B. Control strategy under two failed inverters condition

The second case of study is devoted to analyze the impact of two failed inverters on the operability, of the system described in section II. This degraded mode of the considered quad-inverter, can be divided in two sub-cases. The two alternatives are illustrated respectively by Fig. 8 and Fig. 9. In case of two failed inverters, in two different winding sides (one failed inverter for each windings {1} and {2}), the post fault topology reconfiguration is illustrated by Fig. 8, leading to:

$$\begin{cases} \bar{v}_L^{(1)} = 0 \\ \bar{v}_L^{(2)} = 0 \end{cases} \quad (15)$$

Using the equations (7) with (15), the total motor power  $P$  between the two three-phase windings {1} and {2}, expressed by (8) under healthy condition, becomes:

$$P = \frac{3}{2} (\bar{v}_H^{(1)} \cdot \bar{i}^{(1)} + \bar{v}_H^{(2)} \cdot \bar{i}^{(2)}) \quad (16)$$

As discussed for the previous case, in order to avoid switching losses, only one inverter is used to supply the three phase winding {1}, although the two inverters VSI<sub>H</sub><sup>(1)</sup> or VSI<sub>L</sub><sup>(1)</sup> are healthy. Therefore, the performances of the degraded system (Fig. 8) are exactly the same as for the case of one failed inverter presented in section III-A (Fig. 7).

Subsequently, the corresponding, torque versus speed pattern presented in Fig. 6, can be assumed for this case too. The space vectors generated, and the corresponding area of operation depicted in Fig. 7, can be adopted also for this case. Obviously, under this degraded mode (Fig. 8), the reliability of the system is reduced in comparison to the previous case (Fig. 7). However, this configuration (Fig. 8) allows safe continuity of operation for prolonged time period, without losses or overheating. For the second sub-case, illustrated by Fig. 9, the two healthy inverters are supplying the same winding {1}. Obviously, the two failed ones are disconnected from both, the motor and the corresponding battery sources, leading to:

$$\bar{i}^{(2)} = 0 \quad (17)$$

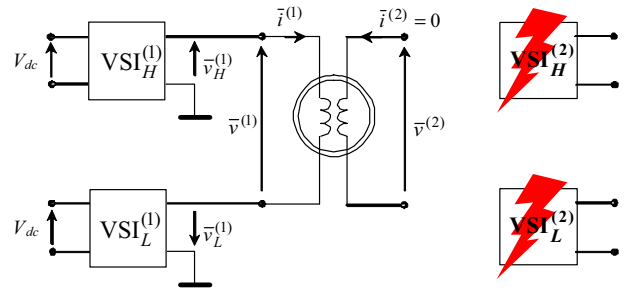


Fig. 9. Equivalent circuit of the whole induction motor drive in terms of three-phase space vectors, under two failed inverters, for one stator windings {2}.

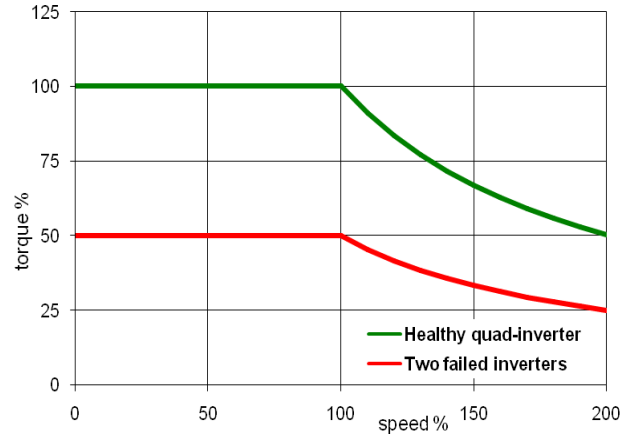


Fig. 10. Torque versus rotor speed under healthy and two failed inverters for the stator windings {2} conditions.

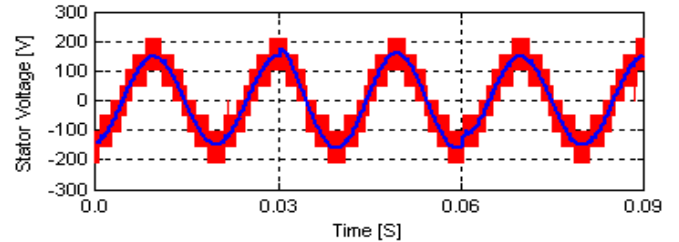


Fig. 11. Stator phase voltage waveform of the three phase winding {1}.

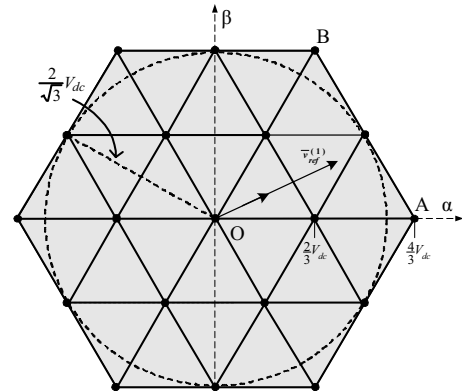


Fig. 12. Plot of voltage space vectors generated by inverters H and L for the stator winding {1}, under two failed inverters, for one stator windings {2}.

Subsequently, using condition (13), the total motor power  $P$  between the two three-phase windings {1} and {2}, expressed by (12) under healthy condition, becomes:

$$P = \frac{3}{2} (\bar{v}_H^{(1)} \cdot \bar{i}^{(1)} + \bar{v}_L^{(1)} \cdot \bar{i}^{(1)}) \quad (18)$$

For this post-fault condition, the system is able to continue the operation, with reduced torque of 50% of the rated capabilities as depicted in Fig. 10. With 50% of the full load torque, the system is able to cover all the speed range, as for a healthy system. This is mainly due to the loss of voltage occurring after the disconnection of the two failed inverters, as depicted in Fig. 9 and expressed by (14).

Once the reference voltage vector  $\bar{v}^{(1)}$  for the two healthy inverters  $VSI_H^{(1)}$  and  $VSI_L^{(1)}$  are determined, the multilevel SVM algorithm is thereby applied. Specifically, under these circumstances, the degraded quad-inverter is able to supply the motor multilevel voltage waveforms. The nine-level waveform of the stator voltage (phase 1) for the first three-phase winding is depicted in Fig. 11 below. Obviously, the switch configurations corresponding to the vector  $\bar{v}^{(1)}$  cannot be applied in an arbitrary sequence, they should be generated by using the developed nearest three vectors approach (NTV) [21].

It is important to note that under this post-fault configuration, the system is able to run for a prolonged long time period without overheating neither on the motor nor on the inverters. Naturally, the same considerations are valuable, even if the inverters  $VSI_H^{(1)}$  or  $VSI_L^{(1)}$  are broken.

### C. Control strategy under three failed inverters condition

The third case of the degraded mode for the qua-inverter investigated in this paper, is devoted to analyze the impact of three failed inverters on the operability of the system. The post-fault topology of the system is illustrated by Fig. 13. It is worth mentioning that the three failed inverters are disconnected from the motor and the corresponding battery sources, leading to:

$$\begin{cases} v_L^{(1)} = 0 \\ i^{(2)} = 0 \end{cases} \quad (19)$$

Consequently, using equations (7) with (19), the total motor power  $P$  between the two three-phase windings {1} and {2}, expressed by (8) under healthy condition, becomes:

$$P = \frac{3}{2} \bar{v}_H^{(1)} \cdot \bar{i}^{(1)} \quad (20)$$

Under post-fault condition, the system is able to continue the operation, with reduced torque of (50% of the rated capabilities) and reduced speed (50% of the rated speed) as depicted in Fig. 14. This is mainly due to the loss of voltage occurring after the disconnection of the three failed inverters, as depicted in Fig. 13 and expressed by (20). For the previously mentioned area of operating conditions, illustrated by Fig. 13, the system is able to operate with similar performances, as for the healthy case (Fig. 2). Eventually, under these conditions, no inverter failure can be tolerated.

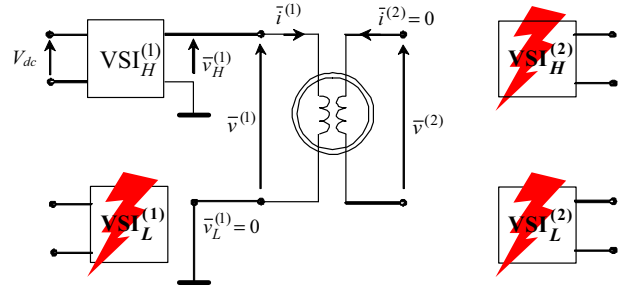


Fig. 13. Equivalent circuit of the whole induction motor drive in terms of three-phase space vectors, under three failed inverters.

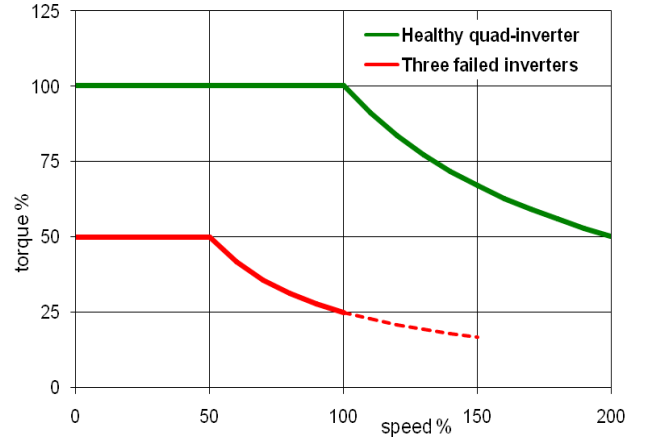


Fig. 14. Torque versus rotor speed under healthy and three failed inverters conditions.

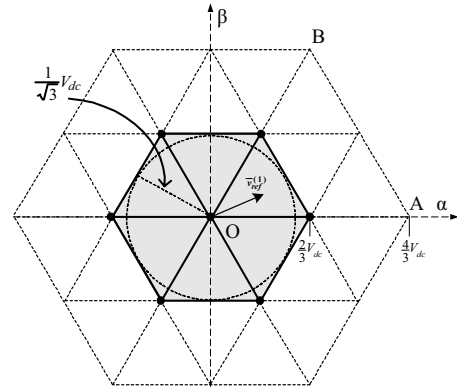


Fig. 15. Plot of voltage space vectors generated by the inverter H of the stator windings {1}, under three failed inverters.

Once the reference voltage vector  $\bar{v}^{(1)}$  for the healthy inverter  $VSI_H^{(1)}$  is determined, the multilevel SVM algorithm is thereby applied. Eventually, under these circumstances, the degraded quad-inverter, allow the supply of the motor as a classical two level inverter.

The corresponding space vector generated and the concerned area of operation were illustrated by Fig. 15. It is important to note that under this post fault configuration, the system is able to run for a prolonged long time period without overheating neither on the motor, nor on the inverters. Naturally, the same considerations are valuable,

under an emergency case, in which the motor must be supplied by only one inverter (the three others are broken).

#### IV. CONCLUSION

Additional degrees of freedom, under post-fault conditions, for high power transport systems, based on a dual three-phase open-ends winding motor, have been analyzed. More specifically, the designed post-fault operating strategies, allow three degrees of freedom, with a balance charge status of the used batteries.

An important issue of the developed fault-tolerant strategy is that allows post-fault operation, where the system is able to run for a prolonged long time period without overheating neither on the motor nor on the inverters.

Numerical implementation of the proposed multi-phase multi-level ac motor drive in different operating conditions shows good agreement with theoretical analysis. The hardware prototype of the whole ac motor drive system is actually under development.

#### V. APPENDIX

##### MOTOR PARAMETERS

Parameter	Value	
$P_{rated}$	kW	8
$I_{S,rated}$	$A_{rms}$	16
$V_{S,rated}$	$V_{rms}$	125
$\omega_{S,rated}$	rpm	$2\pi 50$
$R_S$	$\Omega$	0.510
$R_R$	$\Omega$	0.42
$L_{S1}$	mH	58.2
$L_{R1}$	mH	58.2
$M_1$	mH	56
$p$		2 (pairs)

#### VI. REFERENCES

- [1] A.H. Bonnett, C. Yung, "Increased Efficiency Versus Increased Reliability", *IEEE Ind. App. Mag.*, Vol. 14, N° 1, Jan./Feb. 2008.
- [2] A. Siddique, G. S. Yadava, and B. Singh, "A Review of Stator Fault Monitoring Techniques of Induction Motors", *IEEE Tran. On Ener. Conv.*, Vol. 20, N°. 1, March 2005.
- [3] A. Bellini, F. Filippetti, C. Tassoni, and G. A. Capolino, "Advances in diagnostic Techniques for induction machines", *IEEE Tran. on Ind. Elec.*, Vol.55, N° 12, Dec. 2008.
- [4] E. Levi, "Multiphase electric machines for variable-speed applications," *IEEE Trans. Ind. Electron.*, vol. 55, no. 5, pp. 1893–1909, May 2008.
- [5] G. Grandi, G. Serra, and A. Tani, "General analysis of multiphase systems based on space vector approach," in *Proc. Inter. Power Electronics and Motion Control Conf.*, EPE-PEMC, Portoroz, Slovenia, 30 Aug.–1 Sep. 2006, pp. 834-840.
- [6] J. Rodriguez, S. Bernet, Bin Wu, J.O. Pontt, S. Kouro, "Multilevel voltage-source-converter topologies for industrial medium-voltage drives," *IEEE Trans. Ind. Electron.*, Vol. 54, N° 6, pp. 2930-2945, Dec. 2007.
- [7] L. G. Franquelo, J. Rodriguez, J. I. Leon, S. Kouro, R. Portillo and M. M. Prats, "The age of multilevel converters arrives," *IEEE Ind. Electron. Magazine*, vol. 2, no. 2, pp. 28–39, June 2008.
- [8] O.V. Thorsen and M. Dalva, "A Survey of the Reliability with an Analysis of Faults on Variable Frequency Drives in Industry", *EPE'95*, Sevilla, Spain, pp. 1033-1038, 1995.
- [9] A.L. Julian, G. Oriti, "A comparison of redundant inverter topologies to improve voltage source inverter reliability," in *IEEE Transactions on Industry Applications*, 2007 (vol. 43), pp. 1371-1378.
- [10] US MIL-HDBK 217F, "Reliability Prediction of Electronic Equipment", Notice 1, 2 Dec. 1991.
- [11] S. Yang, A. Bryant, P. Mawby, X. Dawei, L. Ran and P. Tavner, "An industry-based survey of reliability in power electronic converters", *IEEE Ener. Conv. Cong. and Expo.*, pp. 3151-3157, September 2009.
- [12] S. Yang, D. Xiang, A. Bryant, P. Mawby, Li Ran, and P. Tavner, "Condition Monitoring for Device Reliability in Power Electronic Converters: A Review", *IEEE Trans. Power Electron.*, Vol. 25, N° 11, Nov. 2010.
- [13] Y. Zhao, T.A. Lipo, "Space vector PWM control of dual three-phase induction machine using vector space decomposition, " *IEEE Trans. on Ind. Applicat.*, Vol. 31, N° 5, pp. 1100-1109, Sept./Oct. 1995.
- [14] G. Grandi, A. Tani, G. Serra, "Space vector modulation of six-phase VSI based on three-phase decomposition", *19<sup>th</sup> Symposium on Power Electronics, Electrical Drives etc., SPEEDAM'08*, Taormina, June 11-13, 2008, pp. 674-679.
- [15] Y. Kawabata, M. Nasu, T. Nomoto, E.C. Ejiogu, T.Kawabata, "High-efficiency and low acoustic noise drive system using open-winding AC motor and two space-vector-modulated inverters, " *IEEE Trans. on Ind. Electronics*, Vol. 49, no. 4, August 2002, pp. 783-789.
- [16] J. Kim, J. Jung, and K. Nam, "Dual-inverter control strategy for high-speed operation of EV induction motors," *IEEE Trans. Ind. Electron.*, vol. 51, no. 2, pp. 312- 320, Apr. 2004.
- [17] R. Kanchan, P. Tekwani, and K. Gopakumar, "Three-level inverter scheme with common mode voltage elimination and dc link capacitor voltage balancing for an open-end winding induction motor drive, " *IEEE Trans. Power Electron.*, vol. 21, N° 6, pp. 1676-1683, Nov. 2006.
- [18] C. Rossi, D. Casadei, G. Grandi, A. Lega, "Multilevel operation and input power balancing for a dual two-level inverter with insulated DC sources", *IEEE Trans. on Industry Applications*, vol. 44, no. 6, Nov/Dec 2008. pp. 1815-1824.
- [19] S. Yang, D. Xiang, A. Bryant, P. Mawby, L. Ran, and P. Tavner, "Condition monitoring for device reliability in power electronic converters - a review", *IEEE Trans. on Pow. Elec.* (accepted for publication).
- [20] R. Bojoi, A. Tenconi, F. Farina, F. Profumo, "Dual-source fed multi-phase induction motor drive for fuel cell vehicles: Topology and control, " *Proc. of 36<sup>th</sup> Power Electronics Specialists Conference, PESC 2005*, June 2005, Recife, Brasil, pp. 2676-2683.
- [21] D.G. Holmes, T.A. Lipo, "Pulse width modulation for power converters: Principles and practice", *IEEE Press/John Wiley*, 2003, pp. 467–469.
- [22] G. Grandi, A. Tani, P. Sanjeevikumar, D. Ostojic, "Multi-phase multi-level AC motor drive based on four three-phase two-level inverters", *20<sup>th</sup> Symp. on Power Electronics, Electrical Drives and Adv. Electrical Motors, SPEEDAM'10*, Pisa, June 14-16, 2010.